iScience, Volume *27*

Supplemental information

Unique activity of a Keggin POM for efficient heterogeneous electrocatalytic OER

Chandani Singh, Dan Meyerstein, Zorik Shamish, Dror Shamir, and Ariela Burg

Section 1. Characterization of sol-gel electrodes and Co-POM

1.1 Electrode structure

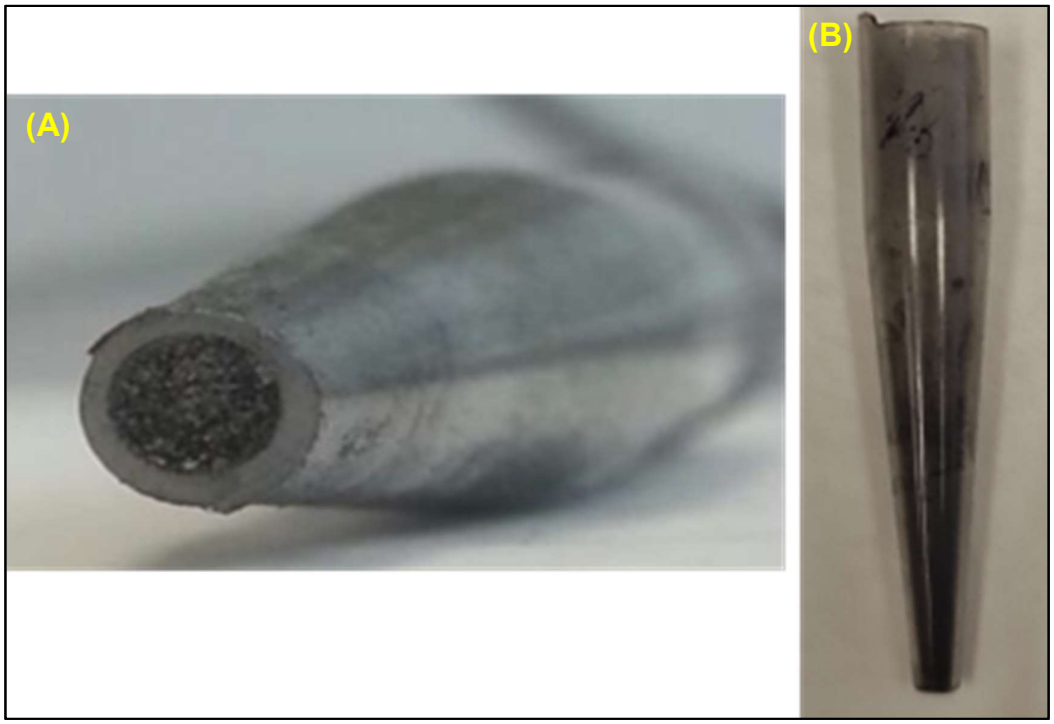

Fig. S1. Sol-Gel electrode entrapped Keggin POM.
(A) Front view of the prepared sol-gel electrode. (B) Side-view of the prepared sol-gel electrode.

1.1 Powder-XRD (PXRD) pattern of Co-POM

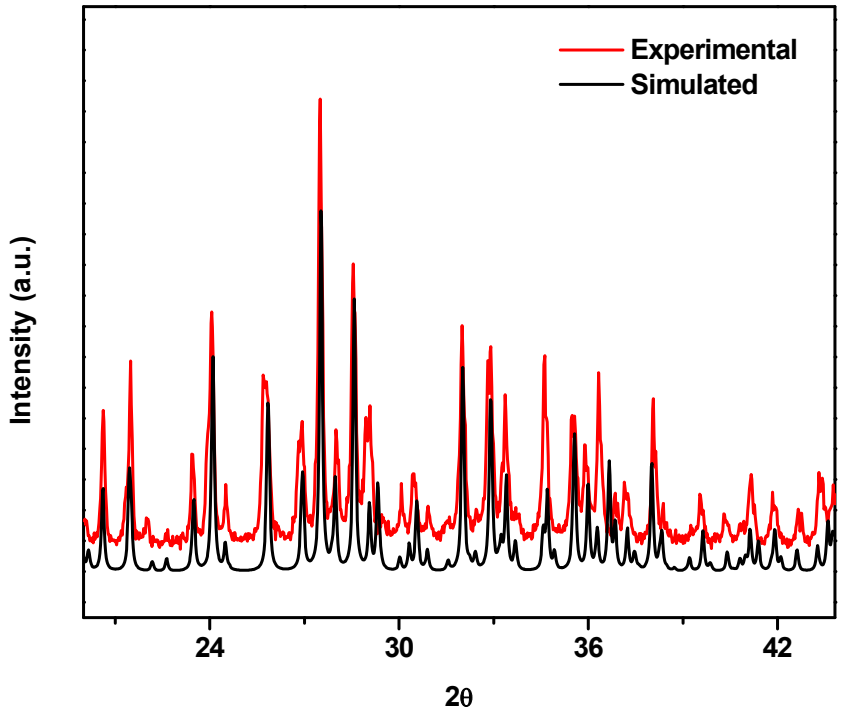

Fig. S2. PXRD pattern of Co-POM compared with its simulated pattern.

1.2. FTIR Analysis

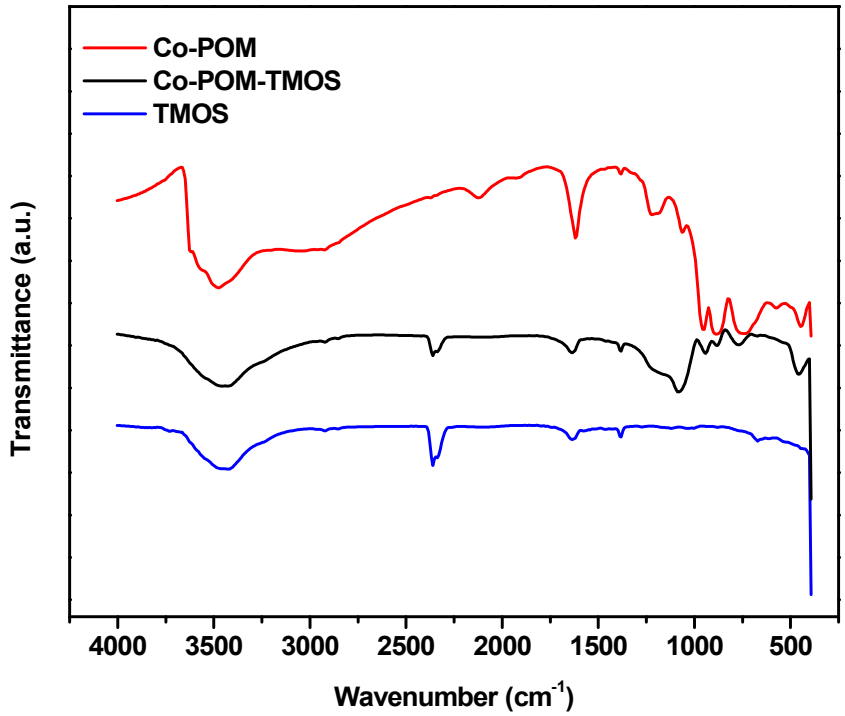

Fig. S3. FTIR pattern of Co-POM-TMOS and TMOS sol gel compared with Co-POM.

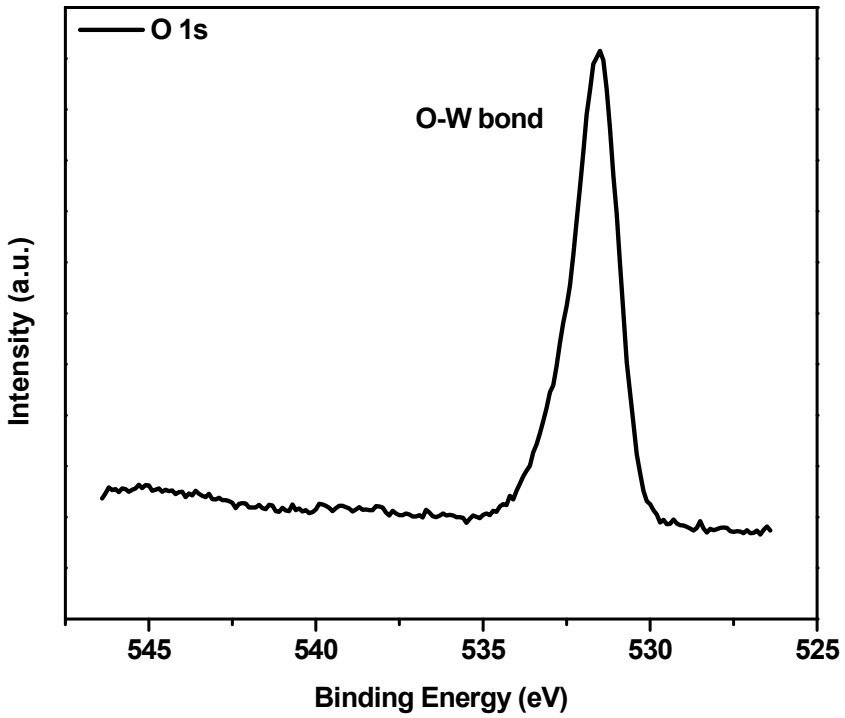

Fig. S4. XPS spectrum of Oxygen in Co-POM.

1.3. Raman analysis

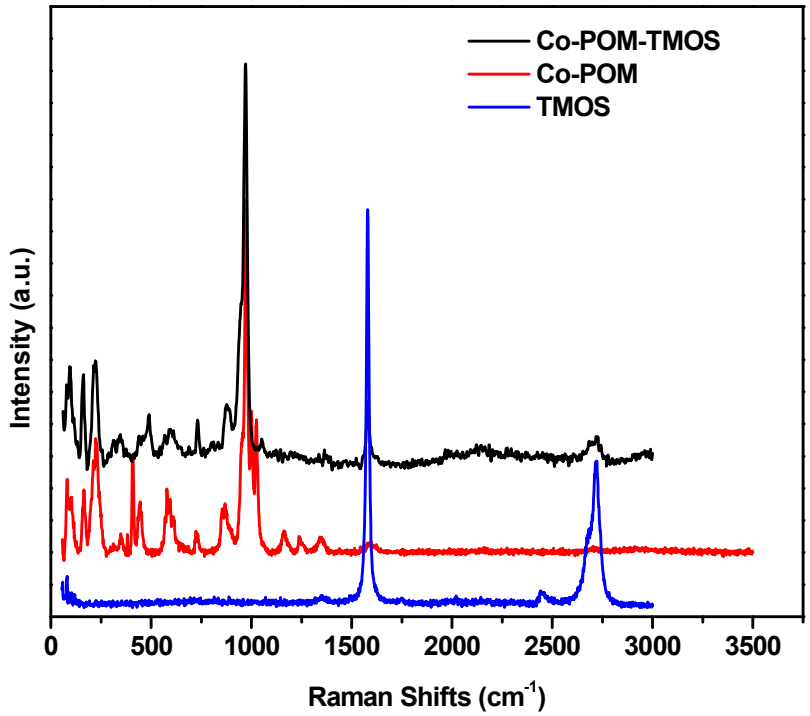

Fig. S5. Raman spectral analysis of Co-POM-TMOS and TMOS sol gel compared with Co-POM. The major peaks in Co-POM are dominated by the terminal W−O stretch at approximately 970 cm^{-1}, Other W−O stretch and bend modes could be spotted at 870 cm^{-1} and 225 cm^{-1}, respectively [1].

Section 2. Electrochemical Studies of Co-POM-TMOS sol-gel electrodes

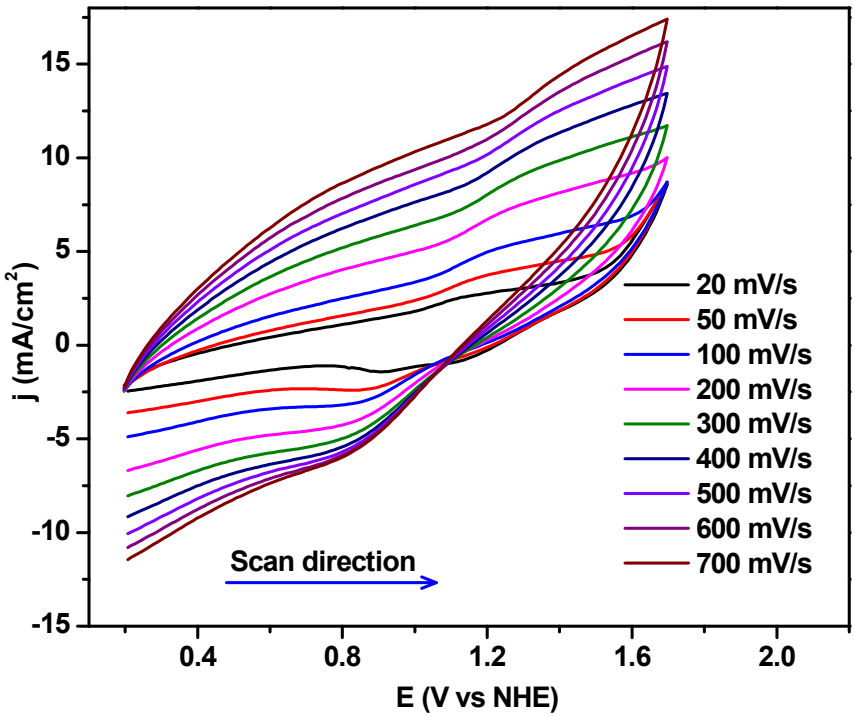

Fig. S6. Cyclic Voltammograms (CVs) recorded for Co-POM-TMOS sol-gel electrode at various scan rates; recorded at 0.2 M $NaClO_4$ pH 2.

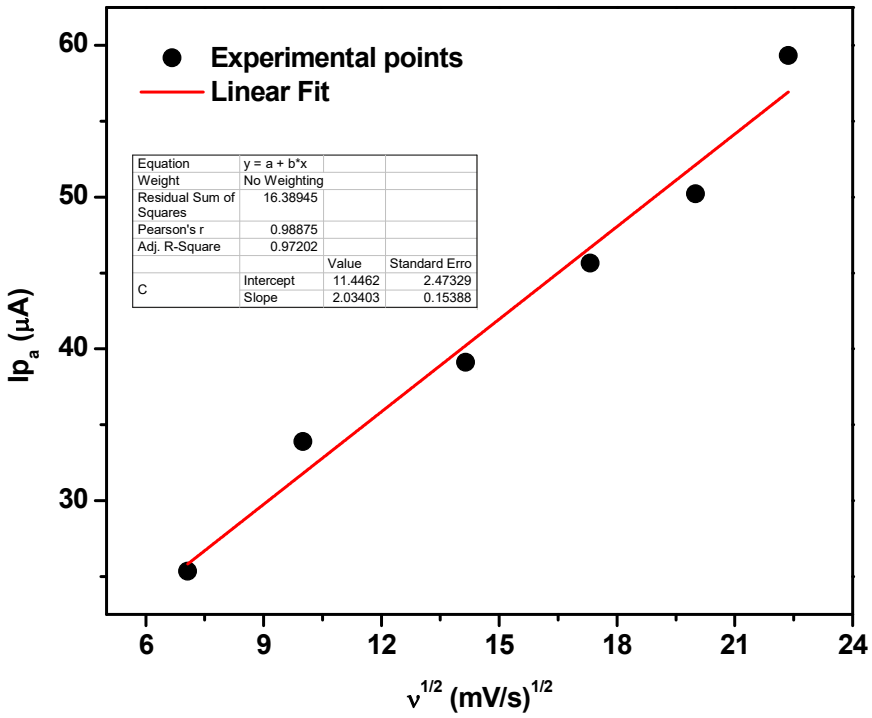

Fig. S7. A plot of anodic peak current (Ip_a) vs. square root of scan rate for Co-POM-TMOS sol-gel electrode.

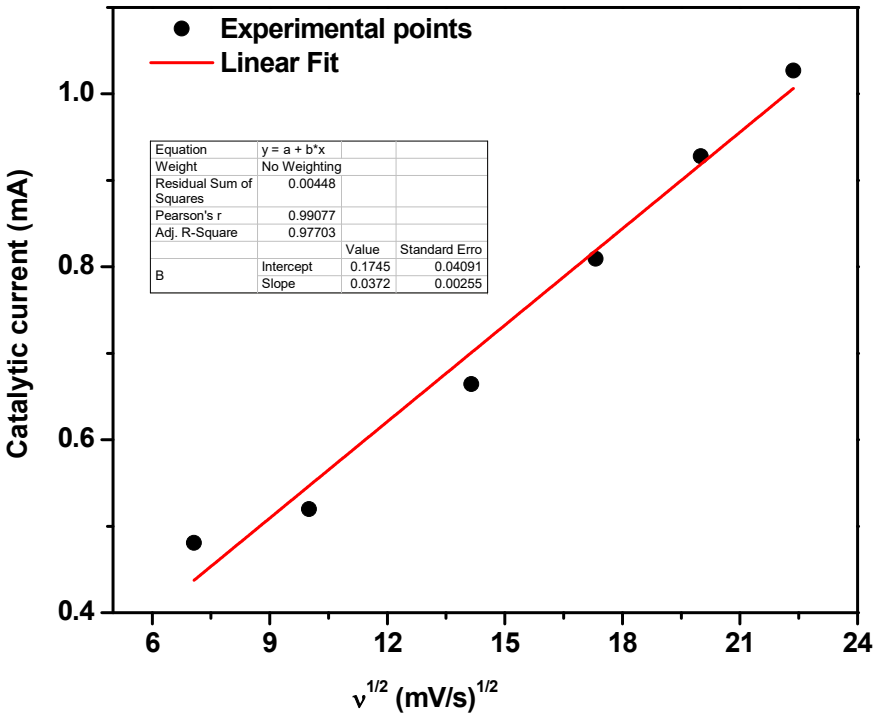

Fig. S8. A plot of cathodic peak current (Ip_c) vs. square root of scan rate for Co-POM-TMOS sol-gel electrode.

Section 3. TOF calculation

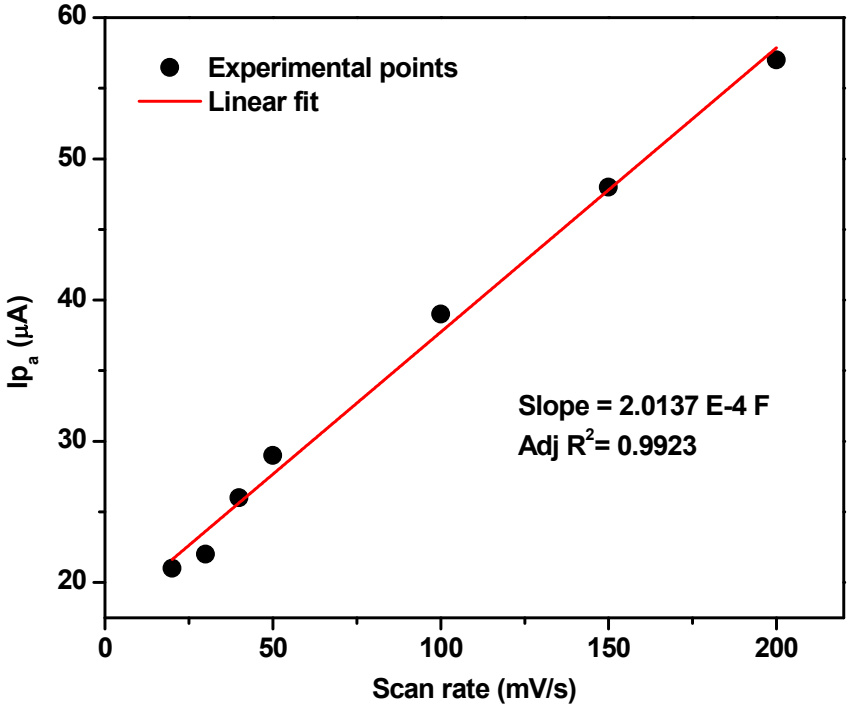

Fig. S9. A plot of anodic peak current (Ip_a) vs. scan rate for Co-POM-TMOS sol-gel electrode.

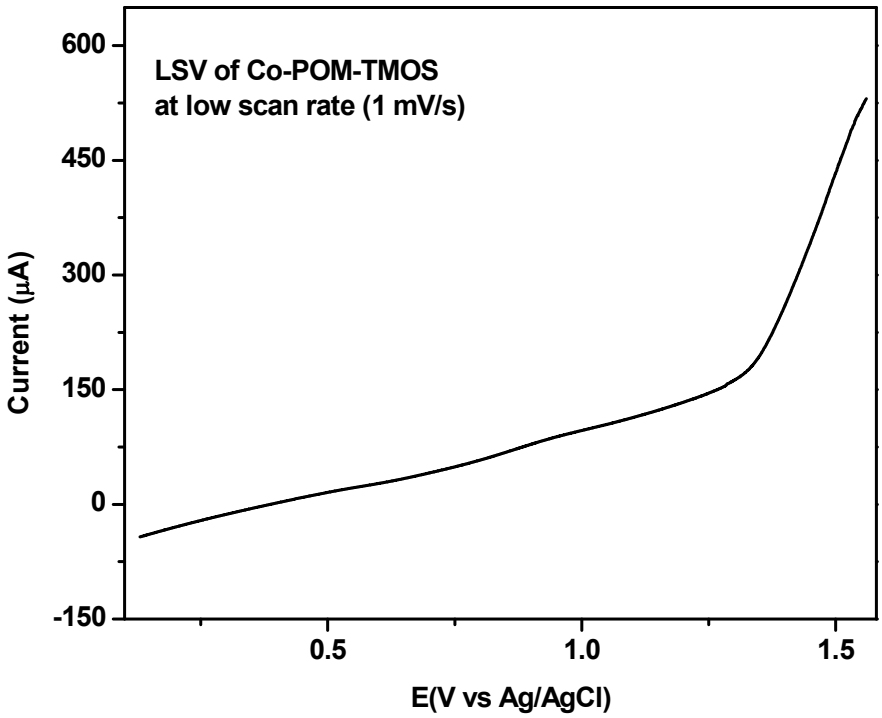

Fig. S10. Linear scan voltammogram (LSV) of Co-POM-TMOS sol-gel electrode recorded at extremely low scan rate (1 mV/s); recorded at 0.2 M $NaClO_4$ pH 2.

Section 4. Calculating Electrochemical Surface area (ECSA) for the sol-gel electrodes:

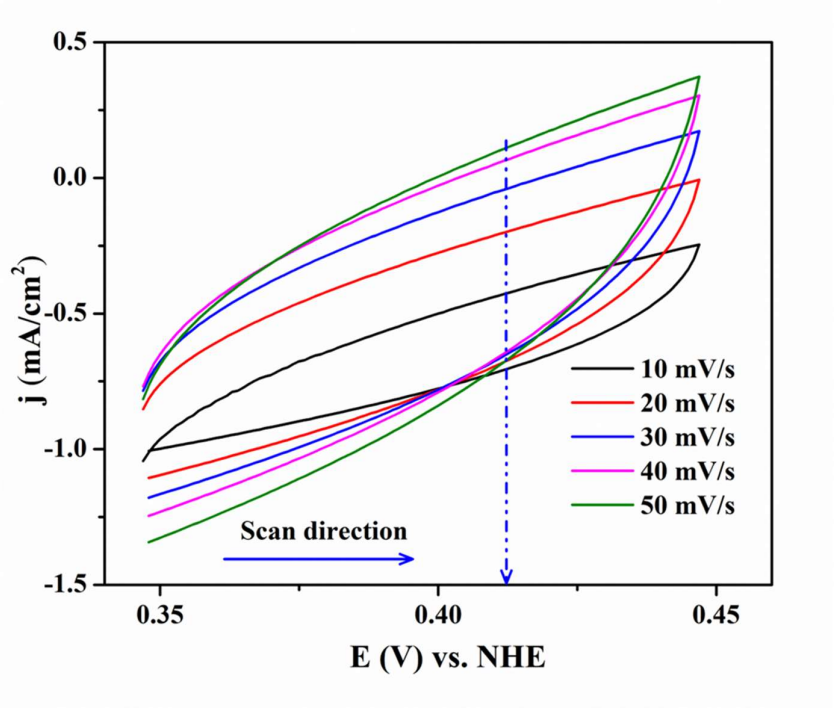

Fig. S11. Cyclic Voltammograms (CVs) recorded for Co-POM-TMOS sol-gel electrode at various scan rates in the non-faradic region (0.35-0.45 V); recorded in 0.2 M $NaClO_4$, pH 2.

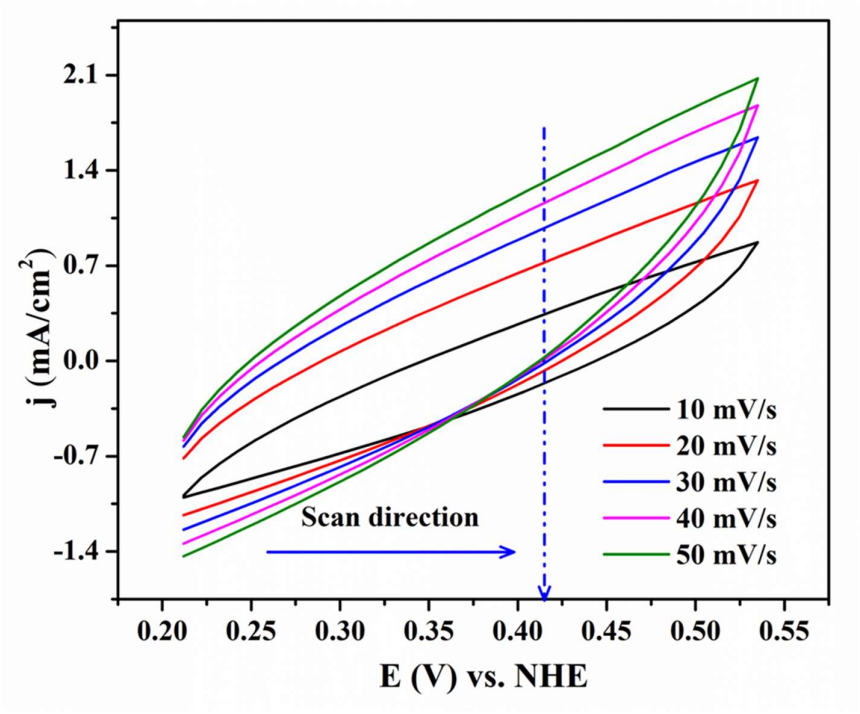

Fig. S12. Cyclic Voltammograms (CVs) recorded for TMOS sol-gel electrode at various scan rates in the non-faradic region (0.35-0.45 V); recorded in 0.2 M $NaClO_4$, pH 2.

Section 5. Characterization of the electrodes post-electrochemical study

Table S1. EDS Analysis of TMOS sol-gel electrode, Co-POM-TMOS sol-gel electrodes before and after the electrochemical study*.

Sample ID	C (%)	Si (%)	O (%)	W (%)
TMOS sol-gel electrode	89.9	0.9	8.1	--
Co-POM-TMOS sol-gel electrodes after Electrochemical test	86.8	1.4	8.6	0.4
Co-POM-TMOS sol-gel electrodes before the Electrochemical test	89.7	1.7	8.2	0.3

* The instrument error equals to ±2%.

Table S2. ICP analysis of 0.2 M of $NaClO_4$ after CPE measurement for Co-POM-TMOS sol-gel electrode.

W (mg/L)	Co (mg/L)	Si(mg/L)
0.4	0.1	1.3

Table S3. Electrodes composition, which were prepared in this study.

Code	Graphite (g)	TMOS (μL)	Co-POM (g)	WATER (μL)	pH
TMOS	0.15	300	0	600	2
Co-POM-TMOS	0.15	300	3.2	600	2
control Co-POM-TMOS	0	300	3.2	600	2

Section 6. Electrochemical Impedance Spectroscopy

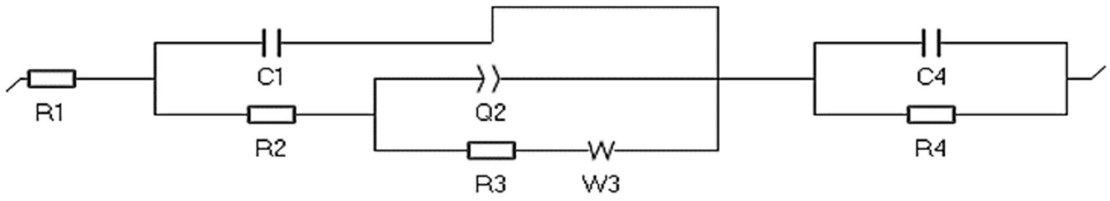

Fig. S13. Equivalent circuit for fitting experimental data of Nyquist plot in figure 5.

Table S4. Parameters of different components of both electrodes as obtained by fitting the Nyquist plot

TMOS -electrode	Co-POM-TMOS electrode
R1 = 354,8 Ohm	R1 = 46,23 Ohm
C1 = 0,153 9e-6 F	C1 = 0,244 4e-6 F
R2 = 56,97 Ohm	R2 = 6,385 Ohm
Q2 = 1,777e-3 F.s^(a - 1)	Q2 = 0,106e-3 F.s^(a - 1)
a3 = 0,272 6	a2 = 0,66
R3 = 60,13e15 Ohm	R3 = 12,14 Ohm
C4 = 18,6e-9 F	s3 = 278,4 Ohm.s^-1/2
R4 = 74,17 Ohm	C4 = 3,079e-3 F
	R4 = 104,5 Ohm

References:

[1] M. Yaqub, J.J. Walsh, T.E. Keyes, A. Proust, C. Rinfray, G. Izzet, T. McCormac, R.J. Forster (2014). Electron Transfer to Covalently Immobilized Keggin Polyoxotungstates on Gold. Langmuir, 30, 4509-4516.